VALIDATION OF A NON-LINEAR FINITE ELEMENT VEHICLE MODEL

USING MULTIPLE IMPACT DATA

Abdullatif K. Zaouk , Nabih E. Bedewi, Cing-Dao Kan, and Dhafer Marzougui

The George Washington University
FHWA/NHTSA National Crash Analysis Center
20101 Academic Way
Ashburn, Virginia 22011
United States of America
Phone: (703)729-8366
Fax: (703)729-8359
e-mail: zaouk@ncac.gwu.edu

ABSTRACT

A detailed multi-purpose finite element model of a 1994 Chevrolet C-1500 pick-up truck was developed at the FHWA/NHTSA National Crash Analysis Center. The model is the first of its kind developed specifically to address vehicle safety issues, including front and side performance, as well as road side hardware design. The former application typically involves large regional deformation with impact durations of no more than 150 msec. The latter encompasses damage along a larger portion of the vehicle, and due to longer interaction time between the vehicle and impacted device coupled with the need to observe post impact dynamics, requires simulations that could last as long as 1 second.

This paper describes the results of a non-linear finite element computer simulation using this model for frontal full barrier and median highway barrier impacts. These simulations are conducted in support of research studies undergoing at the National Highway Traffic Safety Administration (NHTSA) and the Federal Highway Administration (FHWA) to investigate vehicle compatibility, new offset barrier tests, and highway/vehicle safety issues. Full scale vehicle crash tests conducted by NHTSA and FHWA are used for evaluation of the performance of the model. Two tests are compared, a frontal impact with a full rigid wall and a corner impact to a 42-inch Vertical Concrete Median. The comparisons between tests and simulations in terms of overall impact deformation, component failure modes, velocity and acceleration at various locations in the vehicle are presented. Modeling issues including element size, connectivity, and slide line interface of different parts are discussed. In addition, some simulation related hardware and software issues are addressed. The results clearly indicate the model to be consistent with the full scale tests. Additional simulations need to be performed to fully evaluate and validate the model.

INTRODUCTION

Finite element models of vehicles have been increasingly used in preliminary design analysis, component design, and vehicle crashworthiness evaluation, as well as roadside hardware design [1,2,3]. As these vehicle models are becoming more sophisticated over the years in terms of their accuracy, robustness, fidelity, and size, the need for developing multi-purpose models that can be used to address safety issues for a wide class of impact scenarios becomes more apparent[4,5,6,7,8,9].

Several vehicle models have been developed at the U. S. Department of Transportation over the past years. The number of elements ranges in size from five thousand elements based on the Ford Festiva to twenty nine thousand elements based on the Ford Taurus. Different frontal impact scenarios were exercised with these vehicles including rigid narrow objects, full and partial wall barriers, small sign supports and guardrail end terminals. However, the validity of these models in other impact scenarios remains questionable.

Today, with the availability of lower cost super computers based on Symmetric Multi-Processor (SMP) and Massively Parallel Processor (MPP) technologies, simulations of the aforementioned impact cases can be made more elaborate and efficient [10,11]. With these advancements, in the near future, a typical simulation conducted on an SMP or MPP can be performed on a workstation in a similar time. Meanwhile, with the projection that models will continue to grow in size based on the improvement in computation speed, research is needed to improve the modeling abilities and addition of detail and complexity. Furthermore, in order for the vehicle models to be useful for a wide range of impact conditions, the validation needs to be conducted for that whole range.

MODEL DESCRIPTION

Truck Model and its LS-DYNA3D Input File

The finite element model of a 1994 Chevrolet C-1500 pick-up truck was developed at the NCAC for the Federal Highway Administration (FHWA) and the National Highway Traffic Safety Administration (NHTSA). The Chevrolet C-1500 truck is a multi-purpose pickup tuck. The vehicle obtained by the NCAC is a Regular-Cab, Fleetside Long-Box C-1500 with a total length of 5.4 meters (212.6 inches) and a wheelbase of 3.34 meters (131.5) inches. The engine is a 4.3 liter Vortec V6 with Electronic Fuel Injection coupled to a manual transmission with a rear wheel drive configuration. However, several other models exist, such as higher engine capacity, automatic transmission and four wheel drive configuration, with no change in the general geometry. The truck was first disassembled and grouped into seven main groups, the frame, front inner, front outer, cabin, doors, bed and miscellaneous. The three dimensional geometric data of each component was then obtained by using a passive digitizing arm connected to a desktop computer. The surface patches generated from specified digitized data were stored in AutoCAD in IGES format. These IGES files were then imported into PATRAN [13] for mesh generation and model assembly. The model was then translated from PATRAN, which outputs a neutral file, into an LS-DYNA3D [14,15] input file using a translator called HPD [16] developed at the NCAC.

Since this model is used for multi-purpose crash applications, considerable detail was included in the rail frame, and front structures including bumper, radiator, radiator assembly, suspension, engine, side door and cabin of the vehicle. These parts were digitized as detailed as possible, minimizing any loss in the part's geometry. For example, the chassis or main frame, one of the most important structural parts in the truck, was digitized and meshed using two different methods. The first did not include any of the buckling holes while the second included all these holes. In the first case, the model behaved poorly when compared to the test, however the second case behaved as expected. In including these holes, the running time increased. This was caused by the increase in element numbers and the decrease in the element size on the rails. However, there was a significant gain in the truck's behavior.

Another aspect of increasing the model's accuracy, is materials testing. Several coupons from parts such as the engine cradle, fender, hood, bumper, rails, door and door frame were tested to obtain their properties. Two types of tests were conducted on these parts, tension and shear. These tests were conducted at three different rates: slow static, low rate dynamic and high rate dynamic. The properties of these materials will be added to the model in the next phase of the truck model development.

The model consists of 61,776 nodes, 52,541 shell elements, 109 beam elements and 1716 hexahedron elements. The PATRAN neutral file consists of 211 groups, corresponding to the number of element properties, as well as the number of all components. Specifically, the properties of each component are defined by a set of material cards with 4 types of materials being used in the model.

Each of the 211 components is subdivided into either shell elements, beam elements or hexahedron elements. There are two types of shell elements used in the calculation, viz. quadrilateral shell and triangular shell. The formulation of both types of shell elements used for this paper are based on Belytschko-Tsay theory [14,15]. There are only one type of beam and hexahedron elements used in the calculation. The formulations of the beam elements is based on Hughes-Liu theory, while the hexahedron elements uses a one point integration, constant stress formulations.

As mentioned earlier, four LS-DYNA3D material models are used in the truck model. Table 1 lists the material model used along with the number of components. The first column corresponds to the material type number as used by LS-DYNA3D.

Table 1: LS-DYNA3D material models used

No.	Material Type	No. of Components

1	Elastic	25
7	Blatz-Ko Rubber	5
20	Rigid	27
24	Piecewise Linear Isotropic Plastic	154

The elastic material model (material type 1, table 2) was used in components such as the engine, transmission, mounts and radiator. However, in the case of the radiator, a lower density was used.

Table 2: Elastic material model

Elastic	
Density	7.85E-09 t/mm^3
Young's modulus	210,000 N/mm^2
Poisson's ratio	0.3

The Blatz-Ko material model (material type 7, table 3) was used in several mounts such as between the cabin and rails, engine and rails, etc.

Table 3: Blatz-Ko material model

Batz-Ko Rubber	
Density	0.95 t/mm^3
Young's modulus	28 N/mm^2

As seen from table 1, material type 24, the rate-dependent tabular isotropic elastic-plastic material model, is the most commonly used material type. Table 4 includes the values used for this material model in the truck simulation.

Table 4: Piecewise Linear Isotropic Plasticity material model

Piecewise Linear Isotropic Plasticity	
Density	7.85E-09 t/mm^3
Young's Modulus	210,000 N/mm^2
Poisson's Ratio	0.3
Yield Stress	215 N/mm^2
Load Curve	See figure 1
Plastic Strain at failure	∞ (no failure)

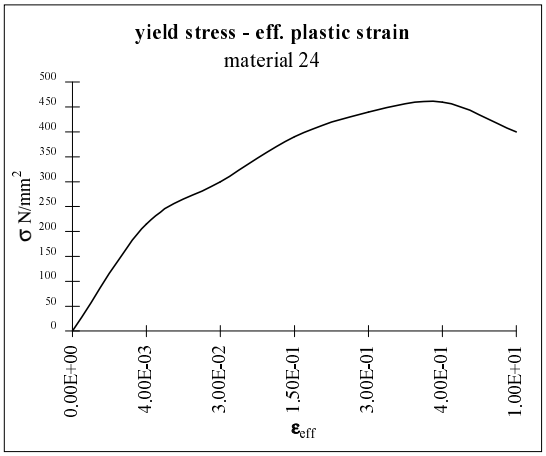

Figure 1: Load curve of stress vs. Effective plastic strain for material 24

In addition, to increase the accuracy of the model, each component is weighed and compared to the simulation weight. This comparison was limited to the accessible parts only. Table 5 lists the major components with the weight comparison between truck and FEM. It should be noted that each of these components is composed of several parts.

Table 5: Weight of various components

Component	Actual Weight (Kg)	FEM Weight (kg)
Door assembly	25.85	26.54
Bumper assembly	19.59	20.49
Fender	14.42	13.38
Hood	25.7	27.09
Radiator assembly	21.99	24.33

The center of gravity location (C.G.) of the model as taken from the truck model was then compared to the center of gravity location obtained from the 42-inch Vertical Concrete Barrier test. Table 6 shows the C.G. location comparison between test and FEM. The C.G. location of the FEM model is reasonable in comparison with the test, this confirms the accuracy of the geometry and weight distribution.

Table 6: Center of gravity location

	X (mm)	Y (mm)	Z (mm)
FEM	-2220.00	-19.75	803.00
Test	-2100.00	0.00	690.00

Parts are connected using three different types of connections: slidelines, constrained nodes, or joints. Slideline type-6, discrete node tied to a surface, was used if two close parallel elements needed to be tied together, such as in the case of the rails. Two types of nodal constraint, group nodal constraint and spot weld, were used. Group nodal constraint assigns the same degree of freedom to a group of nodes, forcing all the constrained nodes to move together and in the same direction. The second type of nodal constraint is the spot weld which can be treated as two nodes connected by a rigid beam. The nodes can move in space in translation and in rotation, but cannot translate or rotate relative to each other. Two types of joints, spherical and revolute, were used to connect the front suspension of the truck model. The sliding interface Type-13 in LS-DYNA3D is used for contact

interface in the computation. In slideline type 13 only the slave materials are specified, and the orientation of the slideline segment is of no matter. These materials are checked against each other and against themselves. Because the slideline check demands significant computational power, only the necessary components were included.

Figures 2a, 2b, and 2c show the isometric, top, and bottom views of the single C-1500 truck FE model, respectively. The hood of the truck was removed in Figure 2b for display purposes.

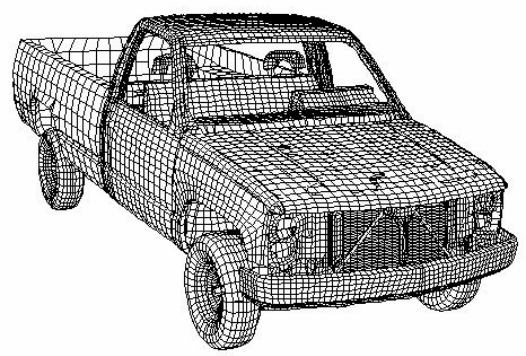

Figure 2a: Isometric view of the truck model

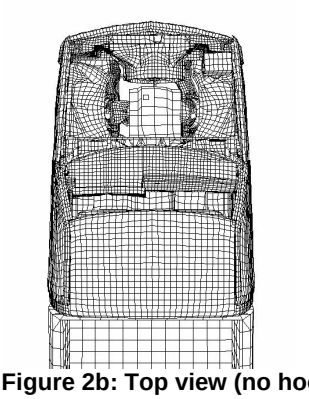

Figure 2b: Top view (no hood)

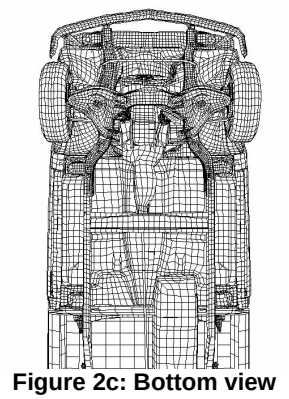

Figure 2c: Bottom view

Creation of Truck to Barrier Models

Two impact scenarios are discussed in this paper. The first is a frontal impact with full rigid wall at an initial velocity of 35 mph (56 kph) (see Figure 3a). The second is a 25 degree corner impact to a 42 inch (1.07 m) vertical concrete median barrier at an initial velocity of 62.5 mph (100 kph) of the truck (figure 3b). The input files for these two impact scenarios were generated using the LS-INGRID [17] pre-processor. In each case, the LS-DYNA3D input files of the truck and corresponding barrier models were combined using LS-INGRID for the specified impact configurations. For the frontal impact with a full rigid wall, sliding interface type-13 was used to model the contact between the truck and the wall. For the 42 inch vertical wall, the geometric contact entity option in LS-DYNA3D was used instead of the sliding interface type-13. New LS-DYNA3D input files for the truck to rigid full barrier and truck to 42-inch vertical barrier were generated and the initial velocities, simulation time step, and termination time were specified.

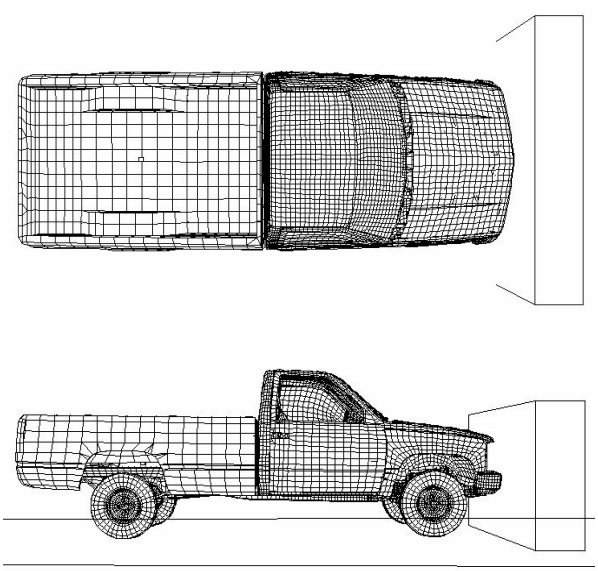

Figure 3a: Frontal impact to a full rigid wall

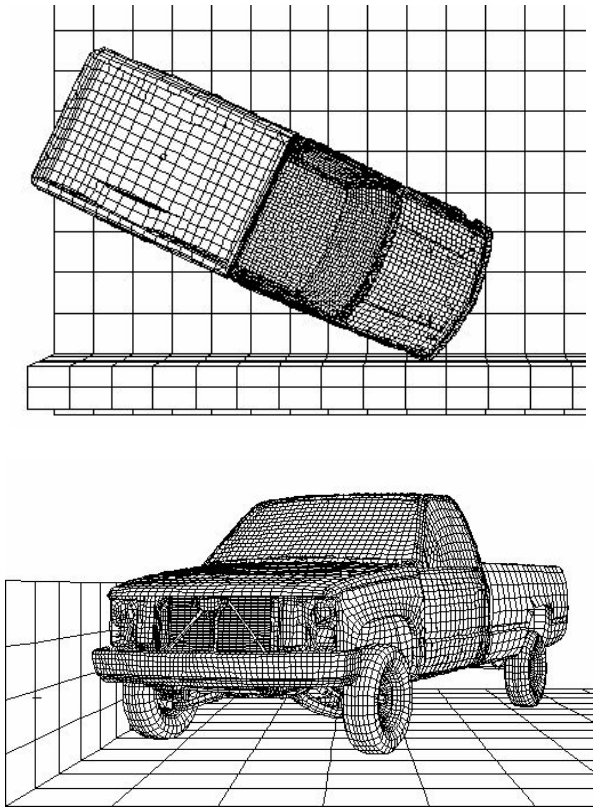

Figure 3b: Corner impact to a 42 inch (1.07 m) concrete median

TEST DESCRIPTION

The frontal impact of the C-1500 pick-up truck with a full rigid barrier was conducted as part of the New Car Assessment Program sponsored by NHTSA under Contract No. DTNH22-90-D-22121, while the corner impact with the 42 inch vertical barrier was conducted as part the National Cooperative Highway Research Program (NCHRP) by the FHWA under Contract No. DTFH61-95-C00136. The detail of the test vehicles and test impact conditions are listed in Tables 6 and 7. In test 1, several transducers were placed throughout the truck, including the engine, brake pad, dashboard, and seats. Data from these transducers are described in the next section along with the comparison to simulations.

Table 7: Description of Test 1

Test Number MN0111	
Test Date	July, 24, 1992
Test Configuration:	Vehicle into Frontal Rigid Barrier with 100% Overlap and 0 Degree Impact Angle
Vehicle:	Chevrolet C-1500 1992 Model Year;
Engine Type:	4.3 liter V6 transverse front mount
Transmission Type:	Automatic
Vehicle Speed:	56.0 KPH (35 mph)

Table 8: Description of Test 2

Test Number 40549-1	
Test Date:	October 19, 1995
Test Configuration:	Vehicle into 42-inch (1.07 m) vertical wall with 25 Degree Impact Angle
Vehicle:	Chevrolet C-2500 1989 Model Year
Engine Type	5.7 V8 transverse front mount
Transmission Type:	Automatic
Vehicle Speed:	100 KPH (62.5 mph)

SIMULATION OUTPUT

The simulations were performed on a Silicon Graphics Power-Challenge system shared memory, SMP super computer consisting of 16 processors. The SMP version of the LS-DYNA3D, version 936 was used. The simulation for the frontal impact was run for 150 milliseconds of impact using 4 processors. The CPU time for the run was 49 hours. For the case of corner impact, the simulation was conducted for 0.4 seconds of impact with a CPU time of 152 hours using 4 processors. In both simulation cases, a fixed time step of 1 microsecond was used. The acceleration records for selected nodal points were outputted every 0.05 milliseconds. These nodal points were chosen based on the sensor locations of the test vehicles. For frontal impact with rigid wall, these positions include: engine, dash-board, and cabin rail while in the 42-inch Vertical Concrete Median the center of gravity (Cg) was added.. An SAE-60 filter was used to reduce numerical noise effects in the simulation for nodal acceleration records, as well as for the test data. The acceleration records are shown along with the test results in the next section.

COMPARISON OF TEST AND SIMULATION

The accuracy and fidelity of the simulation were studied in the following stages: 1) crash deformation profile in the high impact regions; 2) time history records at different locations; 3) energy absorption by different components; and 4) general motion of vehicle. Since the electronic data for the corner impact into the vertical concrete median is under study, stage 3 of the analysis is not yet complete.

Frontal Impact with a Full Rigid Barrier

Crash Deformation Profile in the High Impact Zone-The general deformation at the impact regions can be compared visually from the images captured with the high speed cameras. Figures 4 and 5 show the side and top view of the truck at the initial state and at 39 msec. The 39 msec state is selected because it represents the progression of the deformation on the hood and fenders. These figures also show the same views of the truck but at 60 msec and 90 msec. These states were selected because they represent the stage at which much of the plastic deformation has occurred. It can be observed from the figures that the deformation profiles in hood, fender, and bumper show good correlation between the simulation and the full scale test. Figure 6 shows the bottom view of the truck at the initial state, 39 msec, 60 msec and 90 msec

t = 0 msec t = 39 msec t = 60 msec t = 90 msec

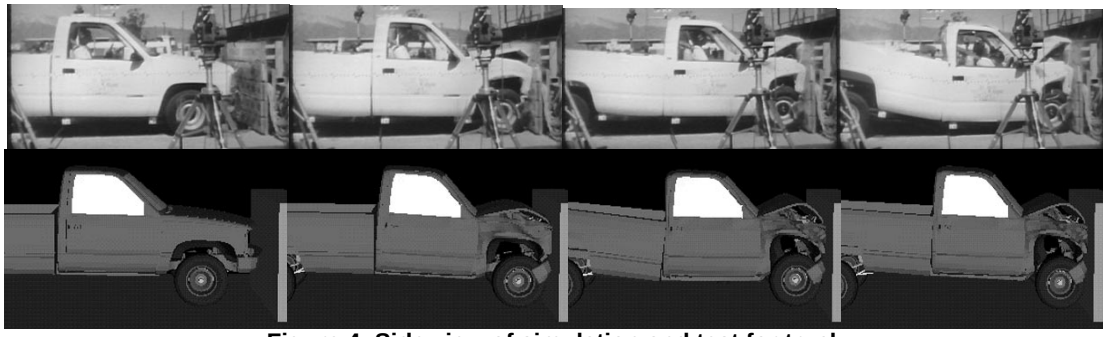

Figure 4: Side view of simulation and test for truck into rigid wall

t = 0 msec t = 39 msec t = 60 msec t = 90 msec

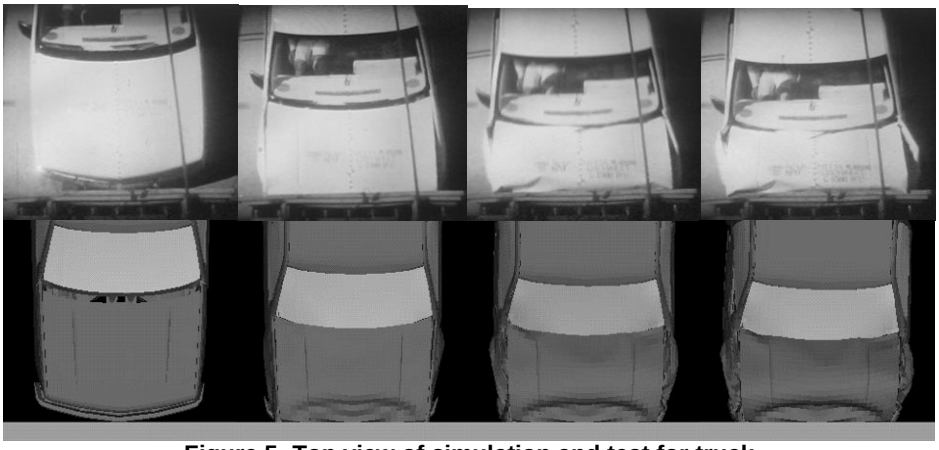

Figure 5: Top view of simulation and test for truck into rigid wall

An arrow was added at the bottom of each image to emphasize the similarity in the plastic deformation of the rails. The general deformation occurring at the bottom of the truck shows a good correlation between simulation and test.

t = 0 msec t = 39 msec t = 60 msec t = 90 msec

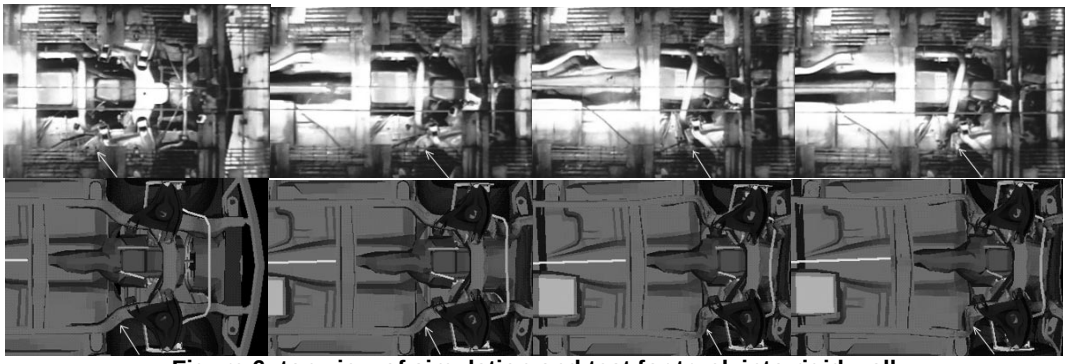

Figure 6: top view of simulation and test for truck into rigid wall

Time History Records at Different Locations - The next level of comparison is the velocity and acceleration time histories at the different locations. Figure 6a shows the comparison of the acceleration record between test and simulation. The accelerometers are located at the bottom of the engine, and on the rear right side of the bench seat. It can be observed that the curve shapes and peak values show good correlation and consistency. The maximum deceleration seen by the engine is 96 g's while that observed in the cabin is 52.3 g's. The errors in prediction are 3.3 % and 16.5 % respectively. Figure 6b is the comparison of velocity time histories of test and simulation taken from the rear left side of the bench seat and the top of the engine. The comparison shows a reasonable agreement between the test and simulation. However, the test is more compliant. This could be attributed to the material properties used in the model, thus emphasizing the importance of material testing and characterization. Variable time steps can be used to reduce simulation error by a factor of 3 [10], particularly in the high impact zone, at the expense of the computational time. For instance, when a variable time step was used, the CPU time for a frontal impact to a rigid wall simulation was 212 hours compared to 49 hours with a fixed time step of 1 microsecond.

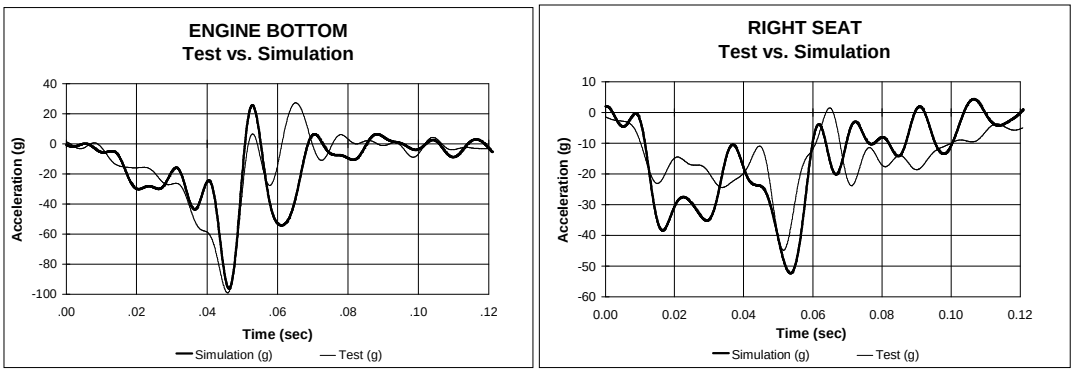

Figure 6a: Acceleration comparison for test and simulation for frontal impact into a rigid wall

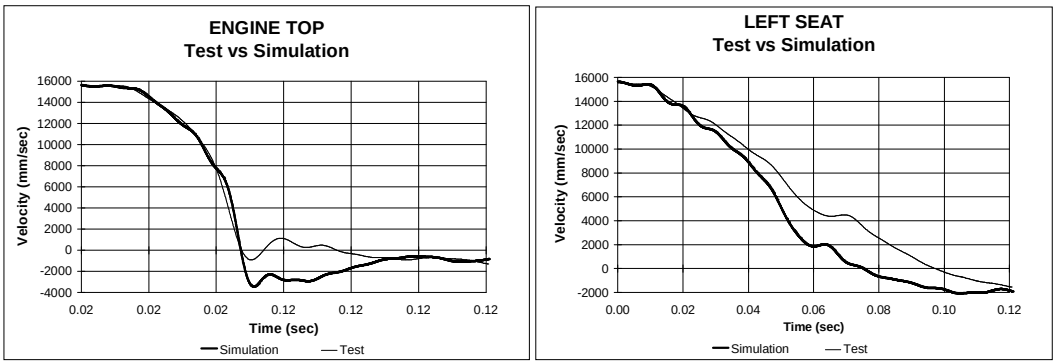

Figure 6b: Velocity comparison for test and simulation of frontal impact to a rigid wall

Energy Absorption by Different Components - It is important to analyze the energy absorption by the different components in the vehicle. This can be obtained in the simulation by computing the material internal energies in the model. The internal energy of the materials is the sum of the plastic strain energy and the elastic strain energy as shown in Figure 7. Tables 8 shows the percent of total energy mitigated through the different components.

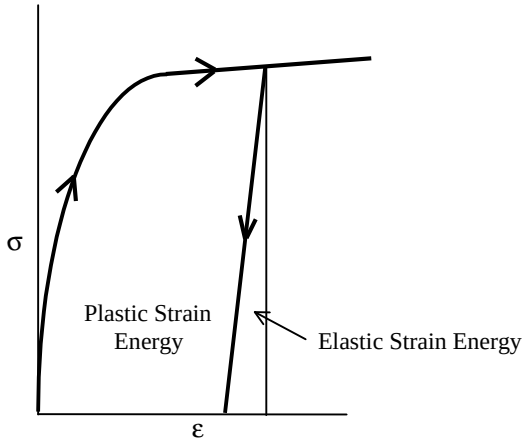

Figure 7: Plastic and elastic strain energies

Table 9: Material Internal Energy for a 35 mph Frontal Impact into a Rigid Wall

Material Parts	Internal Energy (KJoules)	Percentage
Whole Vehicle	214	100%
Rails and its matching structures	93.20	43.55%
Bumper and its matching structures	26.10	12.20%
Engine and its matching structures	23.00	10.75%
Radiator and its matching structures	21.80	10.19%
Toepan and front floor	15.20	7.10%
Hood	10.70	5.00%
Fender	9.80	4.58%
Wheelhouse	1.65	0.77%
Remaining components	12.50	5.84%

The total initial kinetic energy in the model can be computed using the following equation:

$$E = \tfrac{1}{2}mv^2 \qquad (1)$$

Where m represents the mass of the vehicle, and v the velocity. Applying equation 1 for the truck with m=1893.3 Kg, and v = 15.65 m/s results in:

$$E = 231.86 \text{ KJoules}$$

The initial kinetic energy obtained from the simulation is 237 KJoules. The 2.5% difference between the initial kinetic energy computed manually using equation 1 (231.86 KJoules) and the one obtained from the simulation (237 KJoules) is primarily caused by round-off errors and increased mass resulting from using a larger time step than the one dictated by Courant's criteria. This is done to avoid the smallest elements in the model from controlling the time step. The accuracy of the model is not affected by this slight increase, but these elements incur a modest increase in mass such that the Courant criteria is satisfied.

Another important step in the energy balance analysis is to ensure that the conservation of energy condition is satisfied. This can be checked by comparing the final energy and initial energy in the model. The initial energy in this case is mainly attributed to the kinetic energy while the final energy is mainly attributed to internal energy. When comparing the initial kinetic energy and the final internal energy in the model, a difference of 23 KJoules is seen. This portion of energy is basically the kinetic energy left in final state (i.e. the truck impacts the wall and bounces back with a much smaller velocity causing a 23 KJoules of kinetic energy).

The data shown in Table 8 is also important in determining the importance of the respective components to the accuracy and fidelity of the model and the overall simulation. The percent of total energy absorption appears to be consistent with engineering intuition. The results show favorable energy distribution compared with some simulation results of the less detailed model [10].

General Motion of Vehicle -. Observation of the actual crash test of the frontal impact shows good correlation of movements of engine, transmission and drive shaft as shown in Figure 8 for the bottom view. It is noticed that the transmission moved upward in the pictures for both test and simulations emphasized by an arrow. The general similarities between test and simulation can also be noticed in figure 3 at t = 90 msec, where pitching of the flat bed occurs.

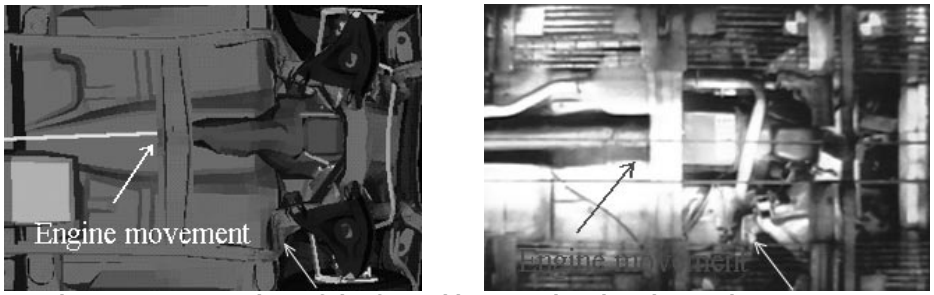

Figure 8: Bottom view of the frontal impact showing the engine movement

Corner impact into a 42-inch vertical concrete barrier

Crash Deformation Profile in the High Impact Zone - The truck tested, C-2500, is a 5.7 Liter V8 with an automatic transmission. This configuration adds a total of 300 Kg to the gross vehicle weight, when compared to the C-1500 equipped with the 4.3 liter Vortec V6. Therefore, weight was added to the model at the engine, transmission, and rear axles. Figures 9 and 10 show the top and front view of the truck at the initial state and at 75 msec. The 75 msec state is selected because it represents the progression of the deformation. These figures also

show the same view of the truck but at 120 msec and 240 msec. These states were selected because they represent the stages at which much of the plastic deformation has occurred. Good correlation can be observed from these figures between test and simulation, such as the door opening on the driver's side and the cabin motion with respect to the bed.

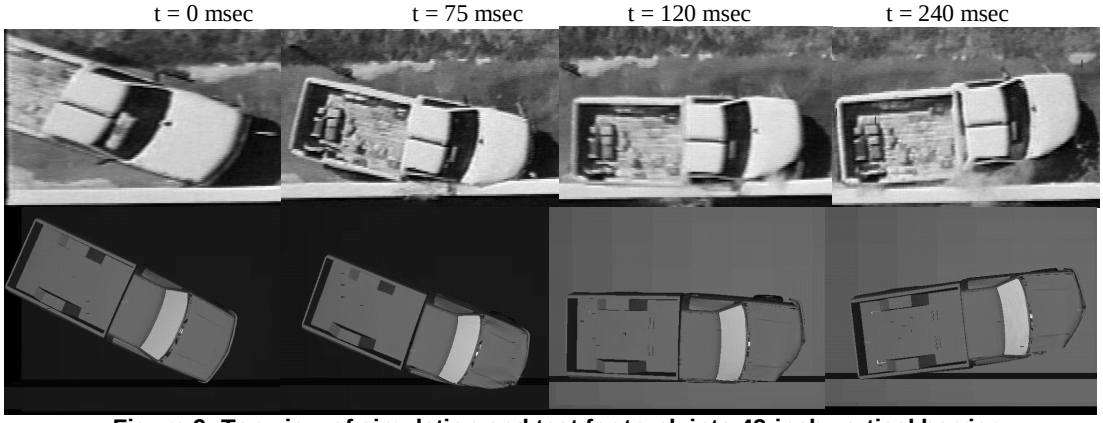

Figure 9: Top view of simulation and test for truck into 42-inch vertical barrier

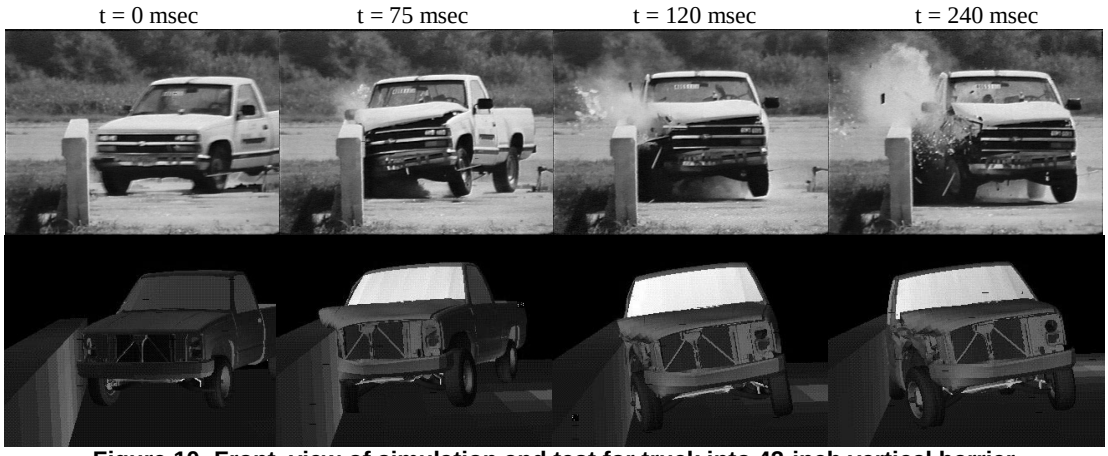

Figure 10: Front view of simulation and test for truck into 42-inch vertical barrier

Time History Records at Different Locations - For the next level of comparison, the velocity time history of test and simulation taken from the truck's center of gravity can be seen in Figure 11.

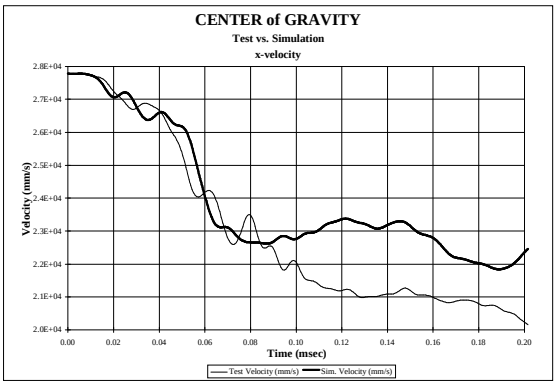

Figure 11: Velocity comparison for test and simulation for corner impact into a rigid barrier

The comparison shows reasonable agreement and, as in the previous case, the test seems to be more compliant. However, no accurate conclusion can be drawn since the data analysis is not complete.

Energy Absorption by Different Components - Table 9 shows the percent of total energy mitigated through the different components. It can be seen that the percent of energy absorption is more distributed than the frontal impact into a rigid wall. This is due to the nature of the impact which causes damage along a larger portion of the truck. The energy absorption appears to be consistent with engineering intuition and the results show good energy distribution.

Table 10: Material Internal Energy for 62 mph Corner Impact into a Rigid Barrier

Material Parts	Internal Energy (KJoules)	Percentage
Whole Vehicle	147.75	100%
Wheels and tires	29.28	19.82%
Rails and its matching structures	26.78	18.13%
Engine and its matching structures	16.11	10.90%
Radiator and its matching structures	15.19	10.28%
Fender	10.06	6.81%
Hood	9.90	6.70%
Bed	9.50	6.33%
Front Suspension	8.65	5.85%
Bumper and its matching structures	8.40	5.69%
Wheelhouse	6.27	4.24%
Toepan and front floor	3.06	2.07%
Rear Suspension	3.00	2.03%
Door	1.70	1.15%

Similar to the full wall case, the initial kinetic energy for the 42 in. vertical concrete median case can be determined using equation 1. The mass of the truck model, however, is slightly higher in this case than that of the previous case (2002 kg as opposed to 1893.3 Kg). This difference in mass is mainly due to the difference in engine size and capacity (5.7L V8 as opposed to 4.3L V6). The initial velocity, 28.69 m/s, is also higher than the one used in the first case (15.65 m/s). Using equation 1, the initial kinetic energy is found to be 797.3 KJoules. This kinetic energy compares reasonably well to the one obtained from the simulation, 800.6 KJoules. The difference is attributed to approximations made in the manual computation of the initial kinetic energy. and increased mass resulting from using a larger time step than the one dictated by Courant's criteria, as discussed previously in the full wall case.

Since no external forces are applied to the system, the total energy in the model must be conserved. This can be verified by comparing the initial and final energies. The total initial energy of the system is equal to the initial kinetic energy (800.6 KJoules) since there are no deformations in the initial state. The total final energy in the sum of the final kinetic energy (650.3 KJoules) and the final internal energy (147.75 KJoules). Comparing the total initial and final energies, it can be concluded that energy in the system is conserved. \

General Motion of Vehicle - As mentioned previously, the validation process is not complete without the overall evaluation of the crash mechanics. Observation of the actual crash test of corner impact shows good correlation of post crash movement as shown in figures 8 and 9. The truck exhibits good rigid body motion; the images show the truck impacting, hugging and then leaving the barrier.

CONCLUSIONS

The simulation results are consistent with the crash tests in terms of different levels of comparison. Some of the problems can be resolved by modeling more components in the cabin interior, including seats, dashboard assembly, and dummies. Furthermore, additional simulations need to be performed using the variable time step integration to separate numerical errors from modeling errors. The model can be further improved by exercising different impact configurations including side impact with the moving deformable barrier (MDB), offset head-on and angle impact with another vehicle, and impact into roadside narrow objects and barriers such as the vertical concrete wall and guardrail.

The simulation results presented in this paper demonstrate a prediction mode for highway barrier impacts based on a model validation with a full frontal barrier impact. These results are preliminary and show a first attempt at such prediction. Further improvement in the model will improve its fidelity and its ability to more accurately predict the behavior under various impact conditions.

As SMP and MPP hardware and software technology becomes more mature, the computational power will enable the simulation of larger and more sophisticated vehicle and occupant models. This, and other such studies, will result in a better understanding of large model development for multiple applications that address vehicle safety and compatibility issues. These applications include frontal, side performance, and new offset barrier tests, as well as roadside hardware design and highway/vehicle safety issues.

ACKNOWLEDGMENT

This research is performed under the contract from U. S. Department of Transportation (DTFH61-92-C-00128). The authors wish to thank Mr. Hansjoerg Schinke for his helpful discussions and assistance with the simulation.

REFERENCES

1. Belytschko, Ted, "On Computational Methods for Crashworthiness," *Proceedings of the 7th International Conference on Vehicle Structural Mechanics*, SAE, Detroit, 1988, pp. 93-102.
2. Cofie, E. and Ray, M. "Simplified finite element vehicle model," *Transportation Research Board Publications, Circular on Computer Simulation,* April, 1994.
3. Varadappa, S., Shyo, S. C., and Mani, A., "Development of Passenger Vehicle Finite Element Model," *Final Report DOT HS 808 145, Department of Transportation,* November 1993, Washington, DC.

4. Perfect, S. and Logan, R. “Evaluation of the Honda Civic Based FE Model,” *Transportation Research Board Publications, Circular on Computer Simulation*, April, 1994.
5. Eskandarian, A., Bedewi, N.E., and Meczkowski, L., “FHWA/NHTSA National Crash Analysis Center,” *Public Roads, A Journal of Highway research and Development*, US DOT, FHWA Office of R&D, 1993.
6. Eskandarian, A., Bedewi, N.E., and Meczkowski, L., “Finite Element Modeling of 4 Lb/Ft. U-Channel Post Sign Support Systems,” *Research and Technology Transporter, a DOT, FHWA Quarterly Accomplishment Report.*
7. Eskandarian, A., Bedewi, N.E., and Marzougui, D., “Finite Element Impact Modeling of Highway Narrow Objects,” *Presented at the Transportation Research Board Annual Meeting/Conference, Session on Computer Simulation of Impacts with Roadside Safety Features*, Washington, DC, January 10-14, 1994.
8. Bedewi, N.E., Omar, T., and Eskandarian, A., “Effect of Mesh Density Variation in Vehicle Crashworthiness Finite Element Modeling,” *Proceedings of the ASME Winter Annual Meeting, Transportation Systems Session*, November 6-11, 1994, Chicago, Ill.
9. Kan, C. D. and Yang, C. “Impact of the Ford Taurus Based FE Model into a Rigid Pole,” *FHWA/NHTSA National Crash Analysis Internal Report.*, August 1994.
10. Bedewi, N.E., Kan, C.D., Summers, S., and Ragland, C., “Evaluation of Car-to-Car Frontal Offset Impact Finite Element Models Using Full Scale Crash Data,” Issues in Automotive safety Technology, SAE Publication SP-1072, pp 212-219, February, 1995.
11. Miller, L., Bedewi, N., and Chu, R., “Performance Benchmarking of LS-DYNA3D for Vehicle Impact Simulation on the Silicon Graphics POWER CHALLENGE” *Presented at the High Performance Computing Asia 95*, Taiwan, October, 1995
12. Schinke, H., Zaouk, A., and Kan, C.D., “Vehicle Finite Element Development of A Chevy C-1500 Truck with Varying Application,” *FHWA/NHTSA National Crash Analysis Internal Report.*, May, 1995
13. *P3/PATRAN USER Manual,* PDA Engineering, Publication 903000, 1993.
14. Hallquist, J.O., *LS-DYNA3D Theoretical Manual*, Livermore Software Technology Corporation, LSTC Report 1018, 1991.
15. Hallquist, J.O., Stillman, D.W., Lin, T.L., *LS-DYNA3D Users Manual* Livermore Software Technology Corporation, LSTC Report 1007, Rev. 2, 1992.
16. Schinke, H.,”HPD, A PATRAN to DYNA Translator,” *FHWA/NHTSA National Crash Analysis Internal Report.*, April, 1995
17. Hallquist, J.O., Stillman, D.W., Lin, T.L., *LS-INGRID Userís Manual*, Livermore Software Technology Corporation, LSTC Report 1008 Rev. 2, 1992.